CONTROL OF DISTRIBUTED PARAMETER SYSTEMS MODELLED BY PARABOLIC VARIATIONAL INEQUALITIES OF THE OBSTACLE TYPE

R. GLOWINSKI[1], R. KUMAR[3], AND J. JANSSON[2,3]

Abstract. We will investigate the numerical solution of the control problem modelled by parabolic variational inequalities. The general point of view adopted in this work has its roots in the work by R. Glowinski[1]. First, we will introduce the model and describe the solution method. In Section 4 and 5, we will discuss the discretization of the model problem and then a conjugate gradient algorithm for solving the problem numerically. Finally we will present numerical results of optimal control problem related to variational inequality.

1. Introduction

Optimal control problems for variational inequalities have been a subject of interest in the optimal control community starting from the 1980s. The motivation for this study comes from two broad interesting applications.

- Reynolds lubrication(thin film)
- Principles of electro-wetting on dielectric(EWOD).

Principle of electro-wetting on dielectric has applications in solar concentrators, mass spectronomy and electrofluidic displays. These problems are fairly complicated from both the analytical and computational point of view. Our goal here is to discuss the solution of control problems for parabolic inequalities of the obstacle type by taking advantage of the penalty based technique. Using penalty, we will be able to approximate the parabolic variational inequalities by nonlinear parabolic equations and then we will apply the fairly classical method discussed in [1].

2. Problem formulation

Let Ω and ω be two bounded domains of $\mathbb{R}^d$, with $d \geq 1$, verifying $\omega \subset \Omega$. The *control problem* that we consider is defined as follows:

$$\begin{cases} Find\ u \in \mathcal{U}\ such\ that \\ J(u) \leq J(v), \forall v \in \mathcal{U}, \end{cases} \tag{2.1}$$

with

$$\mathcal{U} = L^2(\omega \times (0,T)),$$

1991 *Mathematics Subject Classification.* 49M25,49M29,65M60,65K10.

Key words and phrases. Optimal control, Parabolic variational inequality, Conjugate gradient, Finite Element, Adjoint problem.

[1] Department of Mathematics, University of Houston, USA.

[2] Basque center for Applied Mathematics, BCAM, Spain.

[3] KTH, Stockholm, Sweden.

$0 < T < \infty$, and

$$J(\mathbf{v}) = \frac{1}{2} \int\limits_{\omega\times(0,T)} |\mathbf{v}|^2 dxdt + \frac{k_1}{2} \int\limits_{\Omega\times(0,T)} |y - y_d|^2 dxdt + \frac{k_2}{2} \int\limits_{\Omega} |y(T) - y_T|^2 dx \tag{2.2}$$

In (2.2), we assume that: (i) $k_1, k_2 \geq 0$, with $k_1 + k_2 > 0$; (ii) $y_d \in L^2(\Omega \times (0,T))$ and $y_T \in L^2(\Omega)$; (iii) y is defined from v via the solution of the following *parabolic variational inequality*

$$\left\{ \begin{array}{l} y(0) = y_0 (\in K); \\ a.e\ on\ \ (0,T)\ \ , y(t) \in K\ \ and \\ \langle \frac{\partial y(t)}{\partial t}, z - y(t) \rangle + \int\limits_{\Omega} \overline{A} \nabla y(t). \nabla (z - y(t)) \\ \geq \langle f(t), z - y(t) \rangle + \int\limits_{\omega} v(t)(z - y(t)) dx, \forall z \in K, \end{array} \right. \tag{2.3}$$

where (using $\phi(t)$ denote the function $x \to \phi(x,t)$) and:

- $\overline{A} \in (L^\infty(\Omega))^{d\times d}, \exists\ \alpha > 0$ such that $\overline{A}(x)\xi.\xi \geq \alpha|\xi|^2, \forall \xi \in \mathbb{R}^d$, a.e in Ω,
- ·The convex set K is defined by

$$K = \{z | z \in H_0^1(\Omega), z \geq \phi\ \ a.e\ \ on\ \ \Omega\}, \tag{2.4}$$

  with $\phi \in C^0(\Omega) \cap H^1(\Omega)$ and $\phi|_{\partial\Omega} \leq 0$; K is closed and non empty in $H_0^1(\Omega)$ since it contains $\phi^+ (= max(0, \phi))$,

- $\langle \cdot, \cdot \rangle$ denotes the duality pairing between $H^{-1}(\Omega)$(the dual space of $H_0^1(\Omega)$) and $H_0^1(\Omega)$,

- $f \in L^2(0,T; H^{-1}(\Omega))$·

Proving the existence of solution to the elliptic analogues of problem (2.1) is easy; on the other hand, proving the existence of solution to (2.1) is more complicated task since it requires using spaces like $L^p(0,T;X)$, where X is a banach space. Assuming that the solution do exist, we will discuss a method to approximate them.

3. Penalty approximation of the control problem (2.1)

Let ϵ be a positive parameter. We approximate the control problem (2.1) by

$$\left\{ \begin{array}{l} Find\ \ u_\epsilon \in \mathcal{U}\ \ such\ \ that \\ J_\epsilon(u_\epsilon) \leq J_\epsilon(\mathbf{v}), \forall \mathbf{v} \in \mathcal{U}, \end{array} \right. \tag{3.1}$$

with

$$J_\epsilon(v) = \frac{1}{2} \int\limits_{\omega\times(0,T)} |v|^2 dxdt + \frac{k_1}{2} \int\limits_{\Omega\times(0,T)} |y - y_d|^2 dxdt + \frac{k_2}{2} \int\limits_{\Omega} |y(T) - y_T|^2 dx, \tag{3.2}$$

where, in (3.2), k_1, k_2, y_d and y_T are like in (2.2), and where y is obtained from v via the solution of the following *nonlinear parabolic equation*.

$$
\left\{
\begin{array}{l}
y(0) = y_0 (\in K); \\
a.e\ on\ \ (0,T),\ \ y(t) \in H_0^1(\Omega)\ \ and \\
\langle \frac{\partial y(t)}{\partial t}, z\rangle + \int\limits_{\Omega} \overline{A}\nabla y(t).\nabla z dx - \epsilon^{-1} \int\limits_{\Omega} ((y(t)-\phi)^-)^2 z dx = \\
\langle f(t), z\rangle + \int\limits_{\omega} v(t) z dx, \forall z \in H_0^1(\Omega)\cdot
\end{array}
\right. \tag{3.3}
$$

consider the nonlinear operator $\boldsymbol{A}$ defined by

$$
\boxed{\boldsymbol{A}(z) = -\nabla.\overline{A}\nabla z - \epsilon^{-1}((z-\phi)^-)^2} \tag{3.4}
$$

$\boldsymbol{A}$ is continuous from $H_0^1(\Omega)$ into $H^{-1}(\Omega)$; it is also strongly monotone since it verifies

$$
\left\{
\begin{array}{l}
\langle \boldsymbol{A}(y_2) - \boldsymbol{A}(y_1), y_2 - y_1\rangle = \int\limits_{\Omega} \overline{A}\nabla(y_2-y_1)\cdot(y_2-y_1)dx - \\
\epsilon^{-1} \int\limits_{\Omega} [((y_2-\phi)^-)^2 - ((y_1-\phi)^-)^2](y_2-y_1)dx \\
\geq \int\limits_{\Omega} \overline{A}\nabla(y_2-y_1)\cdot\nabla(y_2-y_1)dx \\
\geq \alpha \int\limits_{\Omega} |\nabla(y_2-y_1)|^2 dx,\ \ \forall\ y_1, y_2 \in H_0^1(\Omega).
\end{array}
\right. \tag{3.5}
$$

Due to the monotonicity of the above operator $\boldsymbol{A}$, (3.3) has a unique solution which follows from [3], [4] and [5]. In order to solve the control problem iteratively (using a *conjugate gradient* algorithm for example) it may be most useful to be able to compute the differential $DJ_\epsilon(\mathbf{v})$ of J_ϵ at $\mathbf{v}$. We will find it using perturbation method as discussed in [1].

3.1. **Computation of $DJ_k(v)$:optimality condition.** Suppose that δv is a perturbation of v in $\mathcal{U} = L^2(0,T;H_0^1(\Omega))$ then,

$$
\left\{
\begin{array}{l}
\delta J_\epsilon(v) = \int\limits_{\omega\times(0,T)} DJ_\epsilon(v)\delta v dx dt = \\
\int\limits_{\omega\times(0,T)} v\delta v dx dt + k_1 \int\limits_{\Omega\times(0,T)} (y-y_d)\delta y dx dt + k_2 \int\limits_{\Omega} (y(T)-y_T)\delta y(T) dx,
\end{array}
\right. \tag{3.6}
$$

where, in (3.6) δy is the solution of the following *parabolic equation*(obtained by perturbation of (3.3))

$$
\left\{
\begin{array}{l}
\delta y(0) = 0; \\
a.e\ on\ \ (0,T),\ \ \delta y(t) \in H_0^1(\Omega)\ \ and \\
\langle \frac{\partial}{\partial t}\delta y(t), z\rangle + \int\limits_{\Omega} \overline{A}\nabla\delta y(t).\nabla z dx + 2\epsilon^{-1} \int\limits_{\Omega} (y(t)-\psi)^-\delta y(t) z dx = \\
\int\limits_{\omega} \delta v(t) z dx, \forall z \in H_0^1(\Omega).
\end{array}
\right. \tag{3.7}
$$

Let us consider a function p defined over $\Omega\times(0,T)$, such that

$$
\{p, \frac{\partial p}{\partial t}\} \in L^2(0,T;H_0^1(\Omega)) \times L^2(0,T;H^{-1}(\Omega)), \tag{3.8}
$$

a property which implies $p \in C^0([0,T];L^2(\Omega))$ as in [**?**]. Take $z = p(t)$ in (3.7) and integrate the resulting relation from $t = 0$ to $t = T$; we obtain then

$$\left\{\begin{array}{l} \int\limits_{\Omega} p(T)\delta y(T)dx - \int\limits_{0}^{T}\langle\frac{\partial p(t)}{\partial t},\delta y(t)\rangle dt \ + \int\limits_{\Omega\times(0,T)} \overline{A}^t\nabla p.\nabla\delta y dxdt + \\ 2\epsilon^{-1}\int\limits_{\Omega\times(0,T)}(y-\phi)^-p\delta y dxdt = \int\limits_{\omega\times(0,T)} p\delta v dxdt. \end{array}\right. \tag{3.9}$$

Suppose that p is the (unique) solution of the following linear parabolic equation(the *adjoint equation*)

$$\left\{\begin{array}{l} p(t)\in H_0^1(\Omega),\ \ a.e\ \ on\ \ (0,T), \\ p(T) = k_2(y(T)-y_T), \\ -\langle\frac{\partial p(t)}{\partial t},z\rangle + \int\limits_{\Omega}\overline{A}^t\nabla p(t).\nabla z dx + 2\epsilon^{-1}\int\limits_{\Omega}(y(t)-\phi)^-p(t)zdx \\ = k_1\int\limits_{\Omega}(y(t)-y_d(t))zdx, \forall z\in H_0^1(\Omega). \end{array}\right. \tag{3.10}$$

Taking $z = \delta y(t)$ in (3.10) and combining with (3.6) and (3.9), we obtain

$$\boxed{\int\limits_{\omega\times(0,T)} DJ_\epsilon(v)\delta v dxdt = \int\limits_{\omega\times(0,T)}(v+p)\delta v dxdt} \tag{3.11}$$

that is,

$$\boxed{DJ_\epsilon(v) = v + p|_{\omega\times(0,T)}} \tag{3.12}$$

Remark 3.1.1. The computation of $DJ_\epsilon(v)$ will provide a guideline, when computing (in section 5.4) the time discrete analogue of $DJ_\epsilon(v)$.
Remark 3.1.2. The operator form of (3.10) (a weak formulation is given by)

$$\left\{\begin{array}{l} -\frac{\partial p}{\partial t} - \nabla.\overline{\boldsymbol{A}}^t\nabla p + 2\epsilon^{-1}(y-\psi)^-p = k_1(y-y_d)\ \ in\ \ \Omega\times(0,T), \\ p(T) = k_2(y(T)-y_T) \\ p = 0\ \ on\ \ \partial\Omega\times(0,T), \end{array}\right. \tag{3.13}$$

which is (a relatively) simple linear parabolic equation.
From a practical point of view, the numerical solution of problem requires its *space-time discretization*. The variational approach we took above makes easy the *space approximation* of (3.1), if one uses, for example, the finite element techniques discussed in [1] . The *time discretization* requires a more careful attention and will be discussed in the following section.

4. Time discretization of the control problem

Let $N \geq 1$. We define the time discretization step by $\triangle t = \frac{T}{N}$ and approximate the penalized control problem (3.1) by

$$\left\{\begin{array}{l} Find\ \ \mathbf{u}_\epsilon^{\triangle t}(=\{u^n\}_{n=1}^N)\in\mathcal{U}^{\triangle t} such\ \ that \\ J_\epsilon^{\triangle t}(\mathbf{u}_\epsilon^{\triangle t}) \leq J_\epsilon^{\triangle t}(\mathbf{v})\ \ \forall\mathbf{v}(=\{v^n\}_{n=1}^N\in\mathcal{U}^{\triangle t}, \end{array}\right. \tag{4.1}$$

where in (4.1)

$$\mathcal{U}^{\triangle t} = (L^2(\omega))^N, \tag{4.2}$$

and

$$J_\epsilon^{\triangle t}(\mathbf{v}) = \frac{\triangle t}{2}\sum_{n=1}^{N}\int_\omega |v^n|^2 dx + k_1\frac{\triangle t}{2}\sum_{n=1}^{N}\int_\Omega |y^n - y_d^n|^2 dx + \frac{k_2}{2}\int_\Omega |y^N - y_T|^2 dx, \tag{4.3}$$

where in (4.3), $\{y^n\}_{n=1}^N$ is obtained from $\mathbf{v}$ via the solution of following *time-discrete nonlinear parabolic equation*

$$y^0 = y_0; \tag{4.4}$$

for $n = 1, \ldots, N$, $\{y^{n-1}, v^n\} \to y^n$ via the solution of the following *nonlinear elliptic problem*

$$\begin{cases} y^n \in H_0^1(\Omega), \\ \int_\Omega \frac{y^n - y^{n-1}}{\triangle t} z dx + \int_\Omega \overline{A}\nabla y^n \cdot \nabla z dx - \epsilon^{-1}\int_\Omega ((y^n - \phi)^-)^2 z dx = \\ \langle f^n, z\rangle dx + \int_\omega v^n z dx, \ \ \forall z \in H_0^1(\Omega). \end{cases} \tag{4.5}$$

Using the strict monotonicity and the continuity of the operator

$$z \to \frac{z}{\triangle t} - \nabla\cdot\bar{A}\nabla z - \epsilon^{-1}((z-\phi)^-)^2 : H_0^1(\Omega) \to H^{-1}(\Omega), \tag{4.6}$$

one can easily show that each of the N nonlinear elliptic problems (4.5) has a unique solution.
In order to solve the control problem (4.1) by a conjugate gradient algorithm operating in $\mathcal{U}^{\triangle t}$, We equip $\mathcal{U}^{\triangle t}$ with the inner product $(.,.)_{\triangle t}$ defined (with obvious notation) by

$$(\mathbf{v}, \mathbf{w})_{\triangle t} = \triangle t \sum_{n=1}^{n=N}\int_\omega v^n w^n dx, \tag{4.7}$$

and the corresponding norm. We are going to discuss, just below, the computation of the differential $DJ_\epsilon^{\triangle t}$ of $J_\epsilon^{\triangle t}$. To compute $DJ_\epsilon^{\triangle t}(\mathbf{v})$, we follow the approach taken in Section (5.3) to compute $DJ_\epsilon(\mathbf{v})$. Let us consider thus $\mathbf{v} \in \mathcal{U}^{\triangle t}$ and let us denote by $\delta\mathbf{v}$ a perturbation of $\mathbf{v}$. We have then

$$\delta J_\epsilon^{\triangle t}(\mathbf{v}) = (DJ_\epsilon^{\triangle t}(\mathbf{v}), \delta\mathbf{v})_{\triangle t}, \tag{4.8}$$

and also

$$\delta J_\epsilon^{\triangle t}(\mathbf{v}) = \triangle t\sum_{n=1}^{N}\int_\omega v^n \delta v^n dx + k_1\triangle t\sum_{n=1}^{N}\int_\Omega (y^n - y_d^n)\delta y^n dx + k_2\int_\Omega (y^N - y_T)\delta y^N dx, \tag{4.9}$$

with $\{\delta y^n\}_{n=1}^N$ verifying the following perturbation of (4.4) and (4.5):

$$\delta y^0 = 0; \tag{4.10}$$

for $n = 1, \ldots, N, \{y^{n-1}, v^n\} \to y^n$ via the solution of

$$\begin{cases} \delta y^n \in H_0^1(\Omega), \\ \int\limits_\Omega \frac{\delta y^n - \delta y^{n-1}}{\triangle t} z dx + \int\limits_\Omega \overline{A} \nabla \delta y^n . \nabla z dx + \\ 2\epsilon^{-1} \int\limits_\Omega (y^n - \phi)^- \delta y^n z dx = \int\limits_\omega \delta v^n z dx, \ \ \forall z \in H_0^1(\Omega) \end{cases} \tag{4.11}$$

Let us consider $\{p^n\}_{n=1}^N \in (H_0^1(\Omega))^N$; taking $z = p^n$ in (4.11) we obtain, by summation and after multiplying by $\triangle t$,

$$\begin{cases} \triangle t \sum_{n=1}^N \int\limits_\Omega \frac{\delta y^n - \delta y^{n-1}}{\triangle t} p^n dx + \triangle t \sum_{n=1}^N [\int\limits_\Omega \overline{A} \nabla \delta y^n . \nabla p^n dx + \\ 2\epsilon^{-1} \int\limits_\Omega (y^n - \phi)^- \delta y^n p^n dx] = \triangle t \sum_{n=1}^N \int\limits_\omega \delta v^n p^n dx, \end{cases} \tag{4.12}$$

which implies (by *discrete integration by parts*)that

$$\begin{cases} \int\limits_\Omega p^{N+1} \delta y^N dx + \triangle t \sum_{n=1}^N [\int\limits_\Omega \frac{p^n - p^{n+1}}{\triangle t} \delta y^n dx + \\ \int\limits_\Omega \overline{A}^t \nabla p^n \cdot \nabla \delta y^n dx + 2\epsilon^{-1} \int\limits_\Omega (y^n - \phi)^- p^n \delta y^n dx] = \triangle t \sum_{n=1}^N \int\limits_\omega p^n \delta v^n dx, \end{cases} \tag{4.13}$$

with p^{N+1} still undetermined. Suppose that $\{p^n\}_{n=1}^{N+1}$ verifies the following discrete adjoint equation.

$$p^{N+1} = k_2(y^N - y_T); \tag{4.14}$$

for $n = N, \ldots, 1$, $\{y^n, p^{n+1}\} \to p^n$ via the solution of the following well-posed *linear elliptic problem*

$$\begin{cases} p^n \in H_0^1(\Omega), \\ \int\limits_\Omega \frac{p^n - p^{n+1}}{\triangle t} z dx + \int\limits_\Omega \overline{A}^t \nabla p^n \cdot \nabla z dx + \\ 2\epsilon^{-1} \int\limits_\Omega (y^n - \phi)^- p^n z dx = k_1 \int\limits_\Omega (y^n - y_d^n) z dx, \forall z \in H_0^1(\Omega). \end{cases} \tag{4.15}$$

Taking z = δy^n in (4.15) and combining with (4.14), (4.9) and (4.8), we obtain

$$(DJ_\epsilon^{\triangle t}(\mathbf{v}), \delta \mathbf{v})_{\triangle t} = \triangle t \sum_{n=1}^N \int\limits_\omega (v^n + w^n) \delta v^n dx, \tag{4.16}$$

that is

$$DJ_\epsilon^{\triangle t}(\mathbf{v}) = \{v^n + p^n|_\omega\}_{n=1}^N. \tag{4.17}$$

Remark 4.1.1. The way $DJ_\epsilon^{\triangle t}(\mathbf{v})$ was computed, via the solution of (4.4),(4.5) (4.9), (4.14) and (4.15), suggest that one needs to store $\{y^n\}_{n=1}^N$(in fact its fully discrete analogue obtained by space discretization). Actually a closer look shows that if one operates properly, one needs to store a very small number of snapshots to compute the differential of the cost function.

5. Conjugate gradient solution of the problem 2.1

To solve the above control problem numerically, Polak-Ribiere's conjugate gradient algorithm was implemented since $\mathcal{U}^{\triangle t}$ is a hilbert space for the inner product defined by (4.7) and the associated norm. The Polak-Ribiere's conjugate gradient algorithm reads as follows:

Initialization

$$\mathbf{u}_0(=\{u_0{}^n\}_{n=1}^N) \ \textit{is given in} \ \mathcal{U}^{\triangle t}. \tag{5.1}$$

Solve

$$y_0^0 = y_0; \tag{5.2a}$$

$$\begin{cases} for \ n = 1, \ldots, N, \ \{y_0^{n-1}, u_0^n\} \to y_0^n \ via \ the \ solution \ of \\ y_0^n \in H_0^1(\Omega), \\ \int\limits_\Omega \frac{y_0^n - y_0^{n-1}}{\triangle t} z dx + \int\limits_\Omega \bar{A} \nabla y_0^n . \nabla z dx - \\ \epsilon^{-1} \int\limits_\Omega ((y_0^n - \phi)^-)^2 z dx = \langle f^n, z \rangle + \int\limits_\omega u_0^n z dx, \ \ \forall z \in H_0^1(\Omega), \end{cases} \tag{5.2b}$$

and

$$p_0^{N+1} = k_2(y_0^N - y_T); \tag{5.3a}$$

$$\begin{cases} for \ n = N, \ldots, 1, \ \{y_0^n, p_0^{n+1}\} \to p_0^n \ via \ the \ solution \ of \\ p_0^n \in H_0^1(\Omega), \\ \int\limits_\Omega \frac{p_0^n - p_0^{n+1}}{\triangle t} z dx + \int\limits_\Omega \overline{A}^t \nabla p_0^n . \nabla z dx + \\ 2\epsilon^{-1} \int\limits_\Omega (y^n - \phi)^- p_0^n z dx = k_1 \int\limits_\Omega (y^n - y_d^n) z dx; \forall z \in H_0^1(\Omega) \end{cases} \tag{5.3b}$$

Define $\mathbf{g}_0 \in \mathcal{U}^{\triangle t}$ by

$$\boxed{\mathbf{g}_0 = \{u_0^n + p_0^n|_\omega\}_{n=1}^N} \tag{5.4}$$

if $\frac{\| \mathbf{g}_0 \|_{\triangle t}}{max[1, \| \mathbf{u}_0 \|_{\triangle t}]} \leq$ tol take $\mathbf{u}_\epsilon^{\triangle t} = \mathbf{u}_0$; otherwise, set

$$\mathbf{w}_0 = \mathbf{g}_0 \tag{5.5}$$

For $k \geq 0$, $\{\mathbf{u}_k, \mathbf{g}_k, \mathbf{w}_k\}$ being known with $\mathbf{g}_k$ and $\mathbf{w}_k$ different from 0, compute $\{\mathbf{u}_{k+1}, \mathbf{g}_{k+1}\}$ and if necessary $\mathbf{w}_{k+1}$ as follows:

Descent direction

$$\begin{cases} \rho_k \in \mathbb{R}_+, \\ J_\epsilon^{\triangle t}(\mathbf{u}_k - \rho_k \mathbf{w}_k) \leq J_\epsilon^{\triangle t}(\mathbf{u}_k - \rho \mathbf{w}_k), \forall \rho \in \mathbb{R}_+ \end{cases} \tag{5.6}$$

and set

$$\mathbf{u}_{k+1} = \mathbf{u}_k - \rho_k \mathbf{w}_k \tag{5.7}$$

Testing the convergence and construction of the new descent direction: Solve

$$y_{k+1}^0 = y_0; \tag{5.8a}$$

$$\begin{cases} for\ \ n = 1, \ldots, N,\ \ \{y_{k+1}^{n-1}, u_{k+1}^n\} \to y_{k+1}^n\ \ via\ the\ solution\ of \\ y_{k+1}^n \in H_0^1(\Omega), \\ \int\limits_\Omega \frac{y_{k+1}^n - y_{k+1}^{n-1}}{\triangle t} z dx + \int\limits_\Omega \bar{A} \nabla y_{k+1}^n . \nabla z dx - \\ \epsilon^{-1} \int\limits_\Omega ((y_{k+1}^n - \phi)^-)^2 z dx = \langle f^n, z \rangle + \int\limits_\omega u_{k+1}^n z dx\ \ , \forall z \in H_0^1(\Omega), \end{cases} \tag{5.8b}$$

and

$$p_{k+1}^{N+1} = k_2(y_{k+1}^N - y_T); \tag{5.9a}$$

$$\begin{cases} for\ \ n = N, \ldots, 1,\ \ \{y_{k+1}^n, p_{k+1}^{n+1}\} \to p_{k+1}^n\ \ via\ the\ solution\ of \\ p_{k+1}^n \in H_0^1(\Omega), \\ \int\limits_\Omega \frac{p_{k+1}^n - p_{k+1}^{n+1}}{\triangle t} z dx + \int\limits_\Omega \overline{A}^t \nabla p_{k+1}^n . \nabla z dx + \\ 2\epsilon^{-1} \int\limits_\Omega (y_{k+1}^n - \phi)^- p_{k+1}^n z dx = k_1 \int\limits_\Omega (y_{k+1}^n - y_d^n) z dx,\ \ \forall z \in H_0^1(\Omega). \end{cases} \tag{5.9b}$$

Define $\mathbf{g}_{k+1} \in \mathcal{U}^{\triangle t}$ by

$$\mathbf{g}_{k+1} = \{u_{k+1}^n + p_{k+1}^n | \omega\}_{n=1}^N. \tag{5.10}$$

If $\frac{\| \mathbf{g}_{k+1} \|_{\triangle t}}{max[\| \mathbf{u}_{k+1} \|_{\triangle t}, \| \mathbf{g}_0 \|_{\triangle t}]} \leq tol$, take $\mathbf{u}_\epsilon^{\triangle t} = \mathbf{u}_{k+1}$; otherwise, compute

$$\gamma_k = \frac{(\mathbf{g}_{k+1} - \mathbf{g}_k, \mathbf{g}_{k+1})_{\triangle t}}{\| \mathbf{g}_k \|_{\triangle t}^2}\ \ [Polak - Ribiere's\ \ update] \tag{5.11}$$

and

$$\mathbf{w}_{k+1} = \mathbf{g}_{k+1} + \gamma_k \mathbf{w}_k. \tag{5.12}$$

Do $k + 1 \to k$ and return to (5.40).

The practical implementation of the above algorithm requires:

- The space approximation of the control problem (4.1).
- The solution of the finite dimensional problems approximating (after space approximation) the elliptic problems (5.2b),(5.3b),(5.8b)and (5.9b).
- The solution of the fully discrete analogue of the line search problem (5.6).

Let's assume that $\Omega \subset \mathbb{R}^2$. Concerning the *space approximation* the simplest way to proceed is to approximate ω by a polygonal domain ω_h and then triangulate ω_h using a *finite element triangulation* $\mathcal{T}_h^\omega$. Similarly, we triangulate Ω using finite element triangulation $\mathcal{T}_h^\Omega$ verifying $\mathcal{T}_h^\Omega|_{\bar{\omega_h}} = \mathcal{T}_h^\omega$. Figure 1 verifies the above assumption for triangulation:

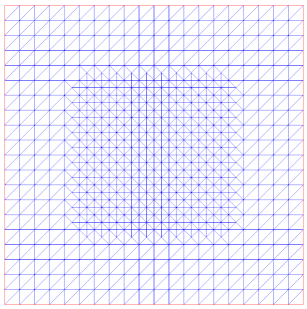

FIGURE 1. Triangulation of $\Omega = (0,1) \times (0,1)$ and $\omega = (\frac{1}{4}, \frac{3}{4}) \times (\frac{1}{4}, \frac{3}{4})$

Following, for example, [1], two simple ways to approximate $L^2(\omega)$ are given by

$$\mathcal{V}_h^0 = \{\mathbf{v} | \mathbf{v} \in L^2(\omega_h), \mathbf{v}|_{\mathcal{K}} \in P_0, \forall \mathcal{K} \in \mathcal{T}_h^\omega\}, \tag{5.13}$$

$$\mathcal{V}_h^1 = \{\mathbf{v} | \mathbf{v} \in C^0(\bar{\omega}_h), \mathbf{v}|_{\mathcal{K}} \in P_1, \forall \mathcal{K} \in \mathcal{T}_h^\omega\}, \tag{5.14}$$

where, in (5.13) and (5.14) $P_0(\mathcal{K})$ and $P_1(\mathcal{K})$ are the space consisting of piecewise constant and linear polynomials respectively on mesh cell $\mathcal{K}$. From the above approximation of $L^2(\omega)$ we approximate $\mathcal{U}^{\triangle t}$ by

$$\mathcal{U}_h^{l,\triangle t} = (\mathcal{V}_h^l)^N, \ \ for \ \ l = 0, 1. \tag{5.15}$$

and we approximate the space $H_0^1(\Omega)$ by

$$\boxed{Z_{0h} = \{z | z \in C^0(\bar{\Omega}_h), z|_{\mathcal{K} \in P_1}, \forall \mathcal{K} \in \mathcal{T}_h^\Omega, z = 0 \ \ on \ \ \partial\Omega_h\}} \tag{5.16}$$

where $\Omega_h = \Omega$ if Ω is a polygonal domain of $\mathbb{R}^2$, and a polygonal approximation of Ω otherwise (we assume all the vertices of $\mathcal{T}_h^\Omega$ belong to $\bar{\Omega}$). It is then quite natural to approximate the space K by

$$K_h = \{z | z \in Z_{0h}, z(P) \geq \phi(P), \forall P \in \sum\nolimits_h\} \tag{5.17}$$

Above, $\sum_h$ is the set of the vertices of $\mathcal{T}_h^\Omega$. We approximate then the penalized control problems (3.1) and (4.1) by

$$\left\{ \begin{array}{l} Find \ \ \mathbf{u}_h^{\triangle t} = \{u^n\}_{n=1}^N \in \mathcal{U}_h^{l,\triangle t} such \ \ that \\ J_{h\epsilon}^{\triangle t}(\mathbf{u}_\epsilon^{\triangle t}) \leq J_{h\epsilon}^{\triangle t}(\mathbf{v}), \forall \ \ \mathbf{v} (= \{v^n\}_{n=1}^N) \in \mathcal{U}_h^{l,\triangle t}, \end{array} \right. \tag{5.18}$$

with

(5.19)

$$J_{h\epsilon}^{\triangle t}(\mathbf{v}) = \frac{\triangle t}{2} \sum_{n=1}^N \int_{\omega_h} |v^n|^2 dx + \frac{k_1 \triangle t}{2} \sum_{n=1}^N \int_{\Omega_h} |y^n - y_{dh}^n|^2 dx + \frac{k_2}{2} \int_{\Omega_h} |y^N - y_{Th}|^2 dx,$$

where in (5.19):

- y_{dh} and y_{Th} are approximations of y_d and y_T(obtained by interpolation in general, if y_d and y_T are continuous functions)
- $\{y^n\}_{n=1}^N$ is obtained from $\mathbf{v}$ via the solution of the following fully discrete non-linear parabolic problem

$$y^0 = y_{0h}; \tag{5.20a}$$

$$\begin{cases} For\ \ n = 1, \ldots, N,\ \ \{y^{n-1}, v^n\} \to y^n\ \ via\ \ the\ \ solution\ \ of \\ y^n \in Z_{0h}, \\ \int\limits_{\Omega_h} \frac{y^n - y^{n-1}}{\triangle t} z dx + \int\limits_{\Omega_h} \overline{A} \nabla y^n . \nabla z dx - \\ \frac{\epsilon^{-1}}{3} \sum_{P \in \Sigma_{0h}} \int\limits_{\Omega} |\omega_P| ((y^n(P) - \phi(P))^-)^2 z(P) dx = \\ \langle f^n, z \rangle_h + \int\limits_{\omega_h} v^n z dx\ \ , \forall z \in Z_{0h}, \end{cases} \tag{5.20b}$$

where in (5.20) (i)y_{0h} is the approximation of y^0 (obtained by interpolation in general if y^0 is a continuous function).(ii) $\sum_{0h}$ is the set of the vertices of $\mathcal{T}_h^\Omega$ which are not located on $\partial\Omega_h$. (iii) ω_p is the polygonal union of those triangles of $\mathcal{T}_h^\Omega$ which have P as a common vertex and $|\omega_P|$ is the measure of ω_P.
The associated adjoint equation reads as:

$$\begin{cases} p^{N+1} \in Z_{0h}, \\ \int\limits_{\Omega_h} P^{N+1} z dx = k_2 \int\limits_{\Omega_h} (y^N - y_{Th}) z dx\ \ , \forall z \in Z_{0h} \end{cases} \tag{5.21}$$

for $n = N, \ldots, 1, \{p^{n+1}, y^n\} \to p^n$ via the solution of following *linear discrete elliptic problem*

$$\begin{cases} p^n \in Z_{0h}, \\ \int\limits_{\Omega_h} \frac{p^n - p^{n+1}}{\triangle t} z dx + \int\limits_{\Omega_h} \overline{A} \nabla p^n . \nabla z dx + \\ \epsilon^{-1} \sum_{P \in \Sigma_{0h}} |\omega_p| ((y^n(P) - \phi(P))^-) p^n(P) z(P) dx = \\ k_1 \int\limits_{\Omega_h} (y^n - y_{dh}^n) z dx; \forall z \in Z_{0h}. \end{cases} \tag{5.22}$$

Concerning the solution of the *nonlinear discrete elliptic problems* (5.20), we advocate Newton method which can be automated by tools in FEniCS. In a nutshell, one can just pass the nonlinear form, the unknown state variable as function object, the essential boundary conditions and the variational form for the Jacobian of the nonlinear form. We will discuss the implementation with minor modification from (5.20) in Appendix.
Finally, concerning the solution of the fully discrete analogue of the line search problem (5.6), we advocate the *Back tracking inexact line search using armijo rule* to readily identify a relatively small interval containing the solution, that is, the fully discrete analogue of the solution ρ^k of the one dimensional optimization problem (5.6). The code used for the line search was a direct implementation of the Pseuso-code in the book by Nocedal and Wright[6].

Remark 5.1.1. The function f^n occurring in the right hand side of (5.20) is a convenient approximation of f at $t = n \triangle t$ and we define $f^n \in H^{-1}(\Omega)$ as $f^n = f(n \triangle t)$. Then, since $\langle ., . \rangle_h$ is an inner product on Z_{0h}, one may define f_h^n by

$$\langle f_h^n, z \rangle_h = \langle f^n, z \rangle, \forall z \in Z_{0h},\ \ f_h^n \in Z_{0h}$$

Discussion: checkpointing. If the forward problem is non-linear, then the solution computed by the forward problem must be available during the execution of the adjoint problem. The adjoint problem depends on the forward solution. If the adjoint problem is solved backwards in time, the forward solution (or the ability to recompute it) must be available for the entire length of forward and adjoint solves. In large simulations, it quickly becomes impractical to store the entire forward solution through time at once. The alternative to storing the forward solution is to recompute them when necessary from checkpoints stored during the forward run; however a naive re-computation would greatly increase the computational burden of the problem to be solved. Therefore, some balance of storage and re-computation is necessary. This problem has been extensively studied in [7] and a similar memory saving devices has been introduced by Griewank [8] in the context of *Reverse-Mode Automatic Differentiation*. The checkpoint can be thought of as a pointers representing the intermediate states of the evolution. To implement the checkpointing, we invoke revolve library. The routine revolve sets the checkpoints in binomial fashion and the intermediate values are being recalculated instead of being recorded. All coding has been done in python.

6. Numerical results

In the following experiments, we will investigate the controllability issues related to variational inequality. For these investigations, we used the data mentioned in Table 1. In the numerical experiments, the desired target y_T, initial condition as y_0 and the source term f, are, for simplicity replaced by approximations, y_{Th}, y_{0h}, f_h. For simplicity we choose $\phi = 0$ and diffusion tensor to be identity matrix for all numerical experiments. The primary reason being the difficulty we faced while generating the form for the nonlinear solver in FEniCS [9].

Table 1. Parameters used to investigate control of parabolic variational inequality

Physical Parameters	Ω	$(0,1)\times(0,1)$
	ω	$(0,1)\times(0,1)$
Penalty parameters	k_1, k_2	$10^2, 10^4, 10^6$
Time discretization parameter	$\triangle t$	10^{-2}

$$\begin{cases} y_T(x,y) = \exp(-\frac{1}{1-x^2} - \frac{1}{1-y^2}) \\ f = |xy - 0.5| + 0.25 \\ y_d = 0 \end{cases} \tag{6.1}$$

6.0.1. ***Numerical results for*** $\omega = (0,1)\times(0,1)$. We choose $\triangle t = 0.01$ as the time-step and total time $T = N \times timestep$, where N is the parameter supplied by the developer. For the first experiment we choose $N = 100$ which implies $T = 1$. In these experiments, we have chosen $u_0 = 0$ as initial guess for control, and k_1, k_2 as the value of the penalty parameter. The corresponding numerical results have been summarized in Table 1, 2, and 3 where u^c and y^c denote the computed

control and corresponding computed state, respectively, and CGIters is the number of iterations required to achieve the convergence of the conjugate gradient algorithm with tolerance, $tol = 10^{-6}$. If the stopping tolerance is too fine then the optimization algorithm performs badly, albeit the relative error decreases. Norm u^c is $\|u^c\|_{L^2(\omega\times(0,T))}$ and Rel. error denotes the relative error between the desired target y_T and computed state $y^c(T)$ which we denote by $\frac{\|y^c(T)-y_T\|_{L^2(\Omega)}}{\|y_T\|_{L^2(\Omega)}}$. First of all we present the controllability result when control is distributed on the whole domain. However, It is not practically realistic to place the control actuators on the whole domain, we therefore investigated the controllability issues for the case when control is distributed on the subset of the domain. We investigated the effect of ϵ on the convergence when the control is distributed on the whole domain. We present the summary of convergence for $k_1 = 10^4$, $k_2 = 10^2$ and different values of ϵ in Table 2. It is not surprising that we get better performance at $\epsilon = 10^{-8}$. It is well known from the proof stated in Mignot et al. [10], Glowinski [2] that the solution y_ϵ of the penalized problem converges to that of variational inequality as $\epsilon \to 0$. However we do not see significant difference in the Rel.error and convergence of the algorithm is not only decided by ϵ. The penalty parameters k_1 and k_2, the desired target y_T and source term f are also key players affecting the Rel. error.

TABLE 2. Summary of convergence for $k_1 = 10^4$, $k_2 = 10^2$, $\omega = (0,1)\times(0,1)$, and T=1

ϵ	k_1	k_2	CGIters	Norm u^c	Rel. error
10^{-2}	10^4	10^2	41	1.0125	0.2551
10^{-3}			40	1.0275	0.2536
10^{-4}			36	1.0377	0.2481
10^{-6}			18	1.2579	0.2421
10^{-8}			17	1.8119	0.1357

We, therefore fix the value of $\epsilon = 10^{-8}$ and study the effect of different values of k_1 and k_2 on the convergence of the conjugate gradient algorithm. We observe that k_1 is the dominating factor concerning the aspect of the optimal control and the convergence behaviour of the algorithm. The performance is better when the value of k_1 is relatively large as compared to the value of k_2, but when we choose the value of k_2 relatively large as compared to the value of k_1 the performance of our conjugate gradient algorithm deteriorates and fails to converge to minimum of J, as soon as the discretization parameters are small enough. The numerical experiments reported indicate that a substancial performance may be obtained after a modest number of iterations. We also investigate the effect of discretization parameter on the convergence of the conjugate-gradient algorithm. We choose $\epsilon = 10^{-8}$, $k_1 = 10^4$, $k_2 = 10^2$ and $T = 1$ to investigate the h-convergence. We observe that as we go on refining the mesh the number of iterations required to achieve the convergence decreases. However the values of L^2 norm of the optimal control and Rel. error show stabilizing behaviour. No dramatic differences in Rel.error when the discretization is refined. We present the visualization of computed state y^c, the desired target y_T for $\omega = (0,1)\times(0,1)$ in Figure 2 and the snapshots of control at different instants of time for this first experiment in Figure 3. We observe that the

TABLE 3. Numerical results with $\epsilon = 10^{-8}$, and $\omega = \Omega = (0,1) \times (0,1)$

ϵ	k_1	k_2	CGIters	Norm u^c	Rel.error
10^{-8}	10^2	10^2	62	1.5243	0.2481
	10^4	10^2	17	1.8119	0.1357
	10^6	10^2	14	0.1182	0.0180
	10^2	10^4	558	15.2588	0.2965
	10^2	10^6	> 1268	-	-

control creates an even temporal distribution. Finally we present the visualization of time evolution of the L^2 norm of the optimal control for different values of k_1 and k_2 in Figure 5.4.

TABLE 4. Numerical results for h-convergence, $T = 1$, $k_1 = 10^4$, $k_2 = 10^2$, $\triangle t = 0.01$, and $\epsilon = 10^{-8}$

h	Norm u^c	CGIters	Rel.error
$\frac{1}{32}$	3.9345	23	0.3161
$\frac{1}{64}$	1.8119	17	0.1357
$\frac{1}{128}$	1.6192	8	0.1124
$\frac{1}{256}$	1.0290	6	0.1048

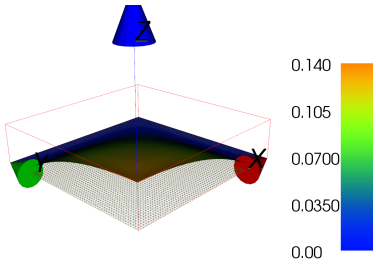

(A) Desired target, y_T

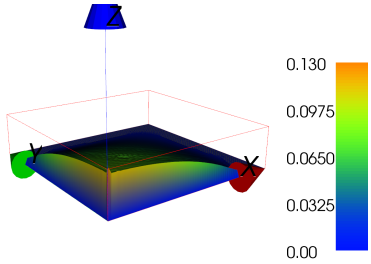

(B) Computed state $y^c(T)$

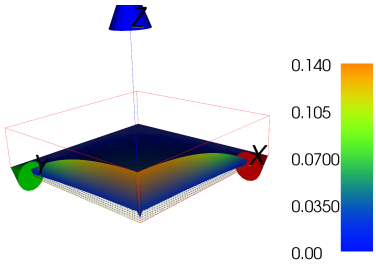

(C) Difference between the desired target, y_T, and computed state $y^c(T)$

FIGURE 2. Visualization of the desired target, y_T, computed state, $y^c(T)$, for $k_1 = 10^4$, $k_2 = 10^2$, $h = \frac{1}{64}$, $T = 1$, and $\omega = \Omega$. The color bar represents the value of function at mesh coordinates.

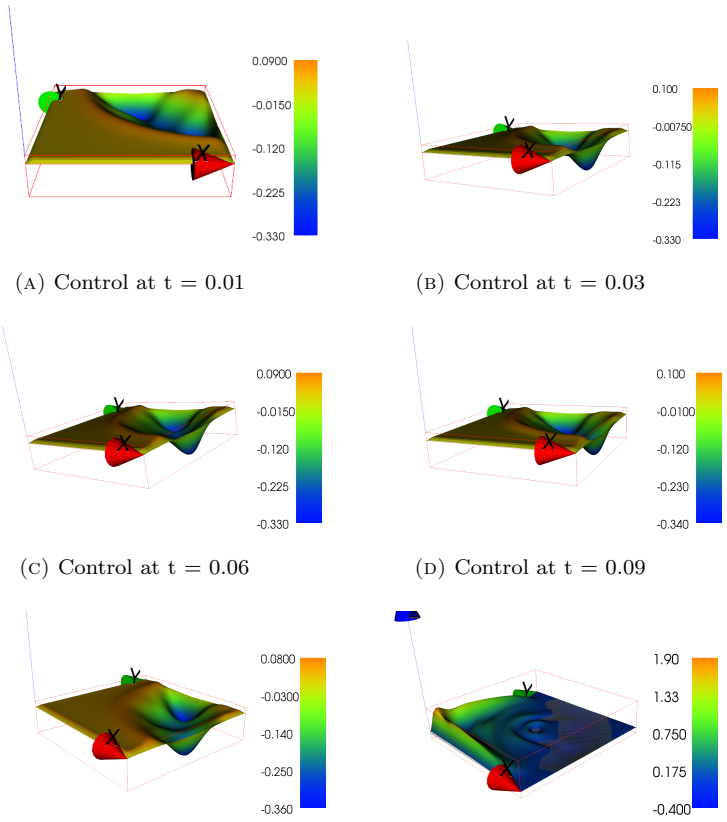

(A) Control at t = 0.01

(B) Control at t = 0.03

(C) Control at t = 0.06

(D) Control at t = 0.09

(E) Control at t = 0.17

(F) Control at t = 0.19

FIGURE 3. Snapshots of the optimal control at different time instants, $k_1 = 10^6$, $k_2 = 10^2$, $\omega = \Omega$, $T = 0.2$, and $\triangle t = 0.01$. The color bar represents the value of the function at mesh coordinates.

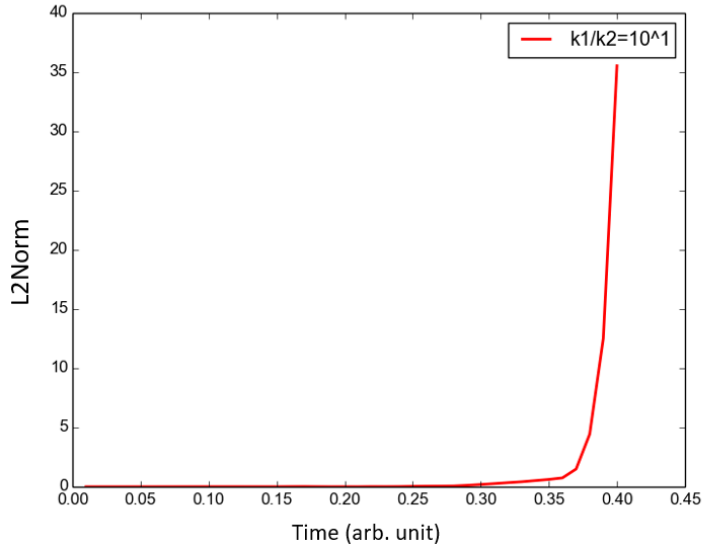

(A) $k_1 = 10^2, k_2 = 10^2$

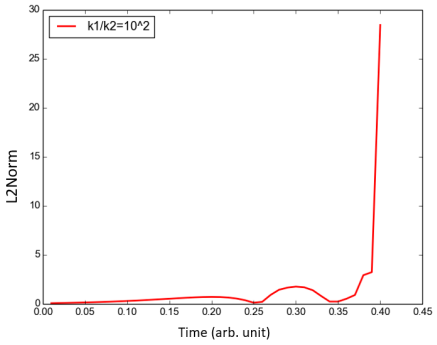

(B) $k_1 = 10^4, k_2 = 10^2$

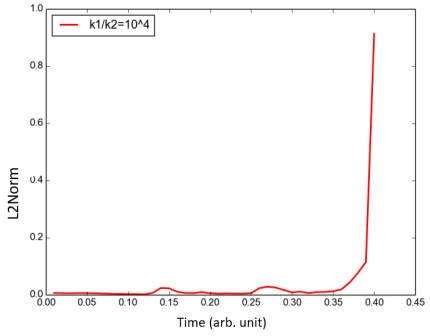

(C) $k_1 = 10^6, k_2 = 10^2$

FIGURE 4. Time evolution of the L^2 norm of the optimal control function for $k_1 = 10^4$ and $k_2 = 10^2$, $T = 0.4$, $\triangle t = 0.01$, and $\omega = \Omega$.

6.0.2. *Numerical results for* $\omega = (\frac{1}{4}, \frac{3}{4}) \times (\frac{1}{4}, \frac{3}{4})$. In this section we present the controllability result when the control is supported on the sub domain $\omega = (\frac{1}{4}, \frac{3}{4}) \times (\frac{1}{4}, \frac{3}{4})$. First, we investigate the effect of epsilon on the controllability for the value of $k_1 = 10^4$ and $k_2 = 10^2$. We choose $tol = 10^{-6}$ for this experiment. We present the summary of convergence results for k_1 and k_2 fixing $\epsilon = 10^{-6}$ in Table 5. In Table 6 we present the effect of discretization parameter h(mesh width of discretization) on the controllability for $k_1 = 10^4$, $k_2 = 10^2$ and time $T = 1$ when control is implemented on the sub-domain. We plot the computed state $y^c(T)$, the desired target y_T and difference between the computed state and desired target in Figure 5. In Figure 6 we present the snapshots of the control at different instants of time. Figure 6(a) and 6(b) is presented differently with an intent to demonstrate the activation of control near zero in the negative y axis. Activation of control near zero in the negative y axis contributes to the low value of the cost of the optimal control.

TABLE 5. Summary of convergence results for $k_1 = 10^4$, $k_2 = 10^2$, $T = 0.5$, $\triangle t = 0.01$, and $h = \frac{1}{64}$

ϵ	k_1	k_2	CGIters	Rel.error	Norm u^c
10^{-2}	10^4	10^2	55	0.4240	1.2504
10^{-3}			54	0.4227	1.2536
10^{-4}			48	0.4215	1.2761
10^{-6}			16	0.4110	1.3785
10^{-8}			14	0.4041	1.6192

TABLE 6. Summary of h-convergence for $\omega = (\frac{1}{4}, \frac{3}{4}) \times (\frac{1}{4}, \frac{3}{4})$, $\triangle t$ = 0.01, T=0.5, $k_1 = 10^4$, and $k_2 = 10^2$

h	Norm u^c	CGIters	Rel.error
$\frac{1}{16}$	3.7868	81	0.4174
$\frac{1}{32}$	2.7387	56	0.4156
$\frac{1}{64}$	1.6192	16	0.4110
$\frac{1}{128}$	1.0290	9	0.4039

We observe that the cost of the control($\|u^c\|_{L^2(\omega\times(0,T))}$) in this case does not show significant difference from the case when the control was distributed on the whole domain. The primary reason for this similarity is the selection of the symmetrical domain which activates the control in similar fashion. We also observe the similar controllability behaviour in case of the sub domain i.e k_1 is the dominating factor. The Rel.error shows stabilizing behaviour and the factor that effects Rel.error are k_1, k_2 and ϵ. The performance is better when we choose high value of $k_1 = 10^6$ and low value of $k_2 = 10^2$. Finally, we present the visualization of the time evolution of the L^2 norm of the optimal control for control supported on sub domain in Figure 7.

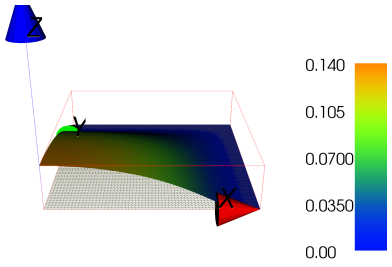

(A) Desired target y_T

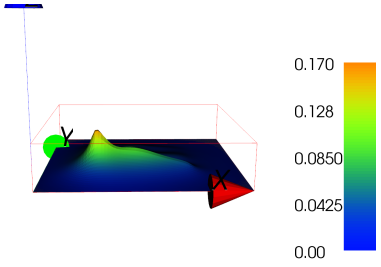

(B) Computed state $y^c(T)$

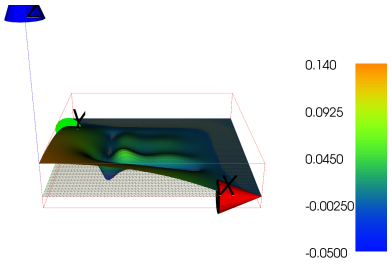

(C) Difference between the desired target, y_T, and computed state $y^c(T)$.

FIGURE 5. Visualization of y^c, y_T and the difference of y^c and y_T for $k_1 = 10^6$, $k_2 = 10^2$, $T = 1$, $h = \frac{1}{64}$, and $\omega = (\frac{1}{4}, \frac{3}{4}) \times (\frac{1}{4}, \frac{3}{4})$. The color bar represents the value of the function at mesh coordinates.

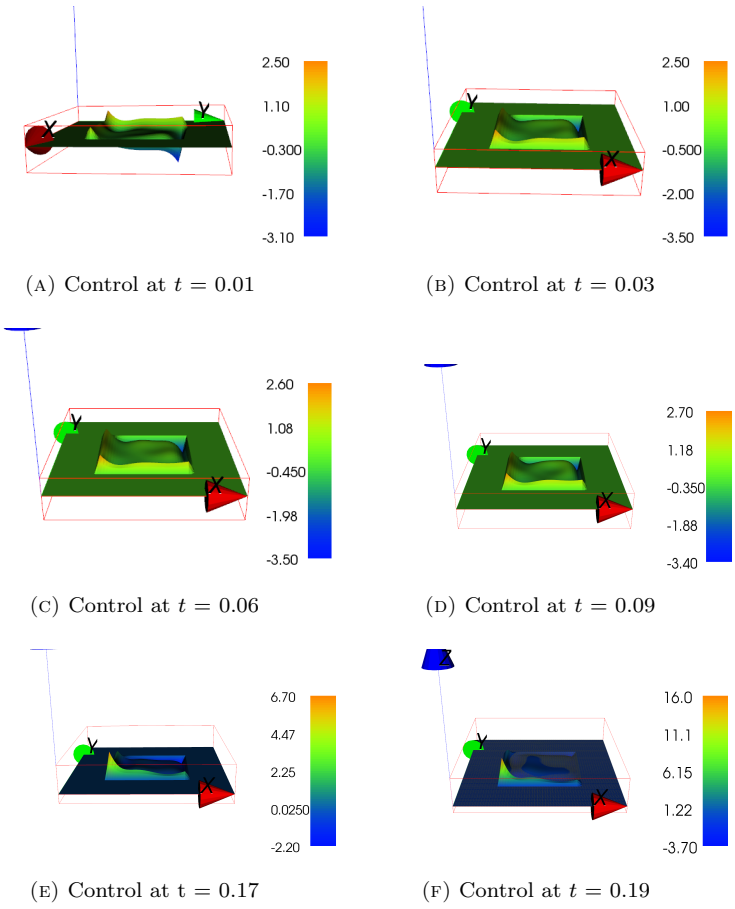

(A) Control at $t = 0.01$

(B) Control at $t = 0.03$

(C) Control at $t = 0.06$

(D) Control at $t = 0.09$

(E) Control at t = 0.17

(F) Control at $t = 0.19$

FIGURE 6. Snapshots of the optimal control at different time instants, $k_1 = 10^6$, $k_2 = 10^2$, $\omega = (\frac{1}{4}, \frac{3}{4}) \times (\frac{1}{4}, \frac{3}{4})$, $T = 0.2$, and $\triangle t = 0.01$. The color bar represents the value of the function at mesh coordinates.

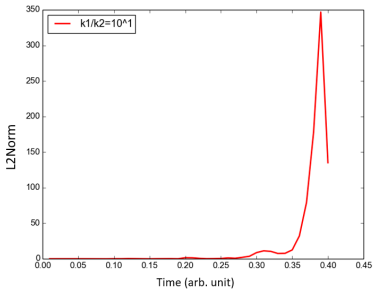

(A) $k_1 = 10^2$, $k_2 = 10^2$

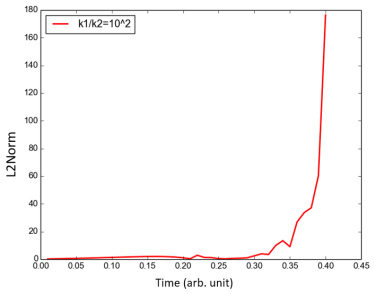

(B) $k_1 = 10^4$,$k_2 = 10^2$

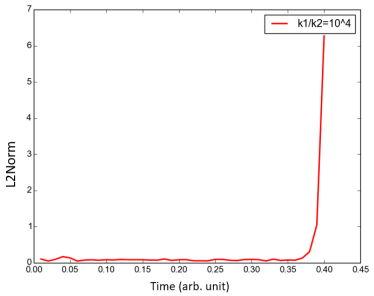

(C) $k_1 = 10^6$, $k_2 = 10^2$

FIGURE 7. Time evolution of the L^2 norm of the optimal control function for $k_1 = 10^4$ and $k_2 = 10^2$, $T = 0.4$, $\triangle t = 0.01$, and $\omega = (\frac{1}{4}, \frac{3}{4}) \times (\frac{1}{4}, \frac{3}{4})$.

We end this section with controllability results for space discretization used in (5.17) to discretize the control space i.e:

$$\mathcal{V}_h^0 = \{\mathbf{v}|\mathbf{v} \in L^2(\omega_h), \mathbf{v}|_{\mathcal{K}} \in P_0, \forall \mathcal{K} \in \mathcal{T}_h^\omega\}, \tag{6.2}$$

The control is assumed to be piecewise constant. More precisely, u is assumed to be constant on each triangle of the triangulation. In this case, each basis function equals unity on exactly one triangle and zero otherwise. We use the data in Table 1 for this experiment. Also the desired target y_T, the source term f and y_d is same as the first experiment. We choose $T = 1$, $\triangle t = 0.01$, $h = \frac{1}{64}$ for this experiment but for visualization purposes we choose small T to demonstrate the activation of control. In order to investigate the effect of the penalty parameter ϵ on the controllability of variational inequality, we choose the value of k_1 and k_2 as 10^6 and 10^2 respectively because of the experience we got after experimenting with previous test cases. The control is supported on $\omega = (\frac{1}{4}, \frac{3}{4}) \times (\frac{1}{4}, \frac{3}{4})$ which is symmetrical around the center. We present our investigation for the effect of ϵ on controllability in Table 7. We observe in Table 8 that the conjugate gradient algorithm takes less iterations to converge if we discretize the control space as mentioned in (5.58). The reason for such behaviour is the appearance of diagonal matrix in the control term after full discretization of the objective functional.

We present the visualization of desired target y_T, computed state $y^c(T)$ and the difference of $y^c(T)$ and y_T in Figure 7. The time evolution of the L^2 norm of the optimal control for different values of k_1 and k_2 is shown in Figure 10. Figure 9 clearly shows the piecewise activation of control when control is supported on the whole domain $\omega = (0, 1) \times (0, 1)$. However, we will not delve into the greater details and only stick to the case where control is distributed on the sub domain $\omega = (\frac{1}{4}, \frac{3}{4}) \times (\frac{1}{4}, \frac{3}{4})$.

TABLE 7. Summary of convergence results with $k_1 = 10^6$, $k_2 = 10^2$, $\omega = (\frac{1}{4}, \frac{3}{4}) \times (\frac{1}{4}, \frac{3}{4})$, h=$\frac{1}{64}$, and T=1

ϵ	k_1	k_2	CGIters	Norm u^c	Rel.error
10^{-2}	10^6	10^2	70	3.3948	0.0174
10^{-3}	10^6	10^2	64	2.9109	0.0174
10^{-5}	10^6	10^2	23	1.6193	0.0174
10^{-8}	10^6	10^2	17	0.6572	0.0064

TABLE 8. Numerical results with $\epsilon = 10^{-8}$, $\omega = (\frac{1}{4}, \frac{3}{4}) \times (\frac{1}{4}, \frac{3}{4})$, T=1, and $h = \frac{1}{64}$

ϵ	k_1	k_2	CGIters	Norm u^c	Rel.error
10^{-8}	10^2	10^2	11	2.1656	0.4758
	10^4	10^2	12	1.3854	0.2962
	10^6	10^2	17	0.6572	0.0064

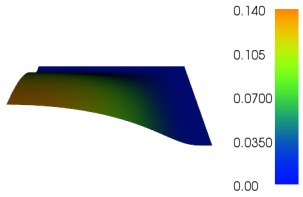

(A) Target function y_T

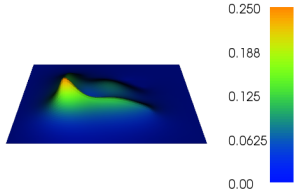

(B) Computed state $y^c(T)$

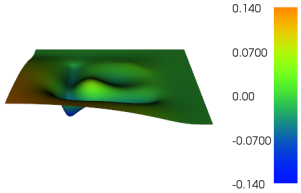

(C) Difference between the target function, y_T, and computed state $y^c(T)$

FIGURE 8. Visualization for $\omega = (\frac{1}{4}, \frac{3}{4}) \times (\frac{1}{4}, \frac{3}{4})$,$T$=0.4, $k_1 = 10^4$, and $k_2 = 10^2$. The color bar indicates the value of the function at mesh coordinates while in the case of the difference it represents the value of the difference taken pointwise.

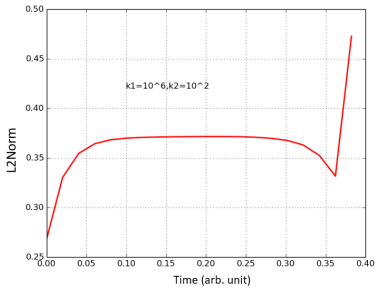

(A) $k_1 = 10^6, k_2 = 10^2$

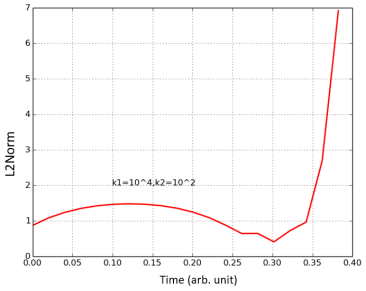

(B) $k_1 = 10^4, k_2 = 10^2$

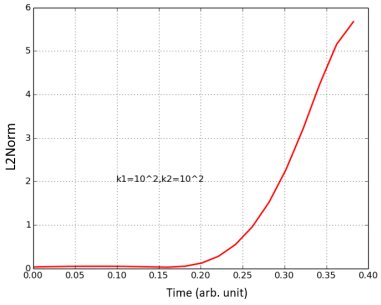

(C) $k_1 = 10^2, k_2 = 10^2$

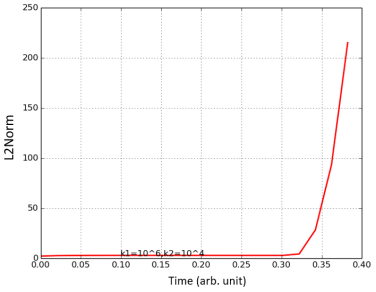

(D) $k_1 = 10^6, k_2 = 10^4$

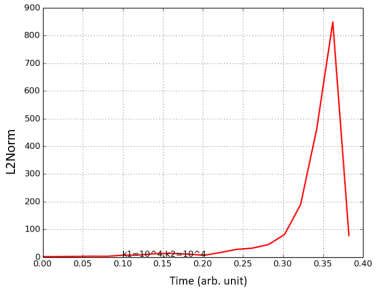

(E) $k_1 = 10^4, k_2 = 10^4$

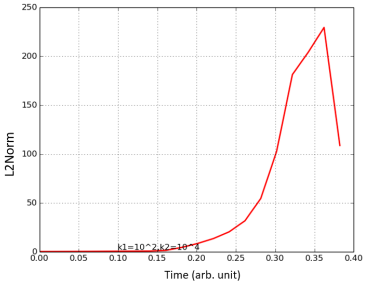

(F) $k_1 = 10^2, k_2 = 10^4$

FIGURE 9. Time evolution of the L^2 norm of optimal control for different values of k_1 and k_2, $\triangle t = 0.01$, $T = 0.4$, and $\omega = (\frac{1}{4}, \frac{3}{4})^2$.

REFERENCES

[1] R. Glowinski; *Exact and Approximate Controllability for Distributed Parameter Systems:A Numerical Approach.* Cambridge University Press **39**, 1-53, 2008.

[2] R. Glowinski; *Numerical Methods for Nonlinear Variational Problems.* Springer-Verlag,New York **50**, 98-140, 1984.

[3] O. A. Ladyzenskaja and V. A. Solonnikov; *Linear and Quasilinear Equations of Parabolic Type* CBMS-NSF Regional Conference Series in Applied Mathematics **2**, 8-48, 1968.

[4] J.L. Lions; *Some Aspects of the Optimal Control of Distributed Parameter Systems.* CBMS-NSF Regional Conference Series in Applied Mathematics, 8-48, 1972.

[5] H. Brezis and A.W. Strauss; *Semi-linear second-order elliptic equations in L^1.* Journal of the Mathematical Society of Japan **4**, 565–590, 1973.
[6] J. Nocedal and S.J. Wright; *Numerical Optimization.* Springer **22**, 59-60, 2000.
[7] M. Berggren; *Optimal Control of Time Evolution Systems:Controllability Investigations and Numerical Algorithms.* Rice University, PhD Thesis **197**, 1850–1864, 1995..
[8] A. Griewank and A. Walther; *Revolve: An implementation of checkpointing for the reverse or adjoint mode of computational differentiation.* ACM Transactions on Mathematical Software. **184**, 19-45, 2000.
[9] M.E. Rognes and D.A. Ham and C.J. Cotter and A.T.T. McRae; *Automating the solution of PDEs on the sphere and other manifolds in FEniCS 1.2.* Optimization theory Appl, Springer, 1-65, 2013.
[10] F. Mignot and J. P. Puel; *Optimal Control in Some Variational Inequalities.* SIAM Journal on Control and Optimization. **22**, 466-476, 1984
[11] S.C. Brenner and L.-Y. Sung; *C^0 interior penalty methods for fourth order elliptic boundary value problems on polygonal domains.* J. Sci. Comput., **22/23**, 83–118, 2005.
[12] S.C. Brenner, K. Wang, and J. Zhao; *Poincaré-Friedrichs inequalities for piecewise H^2 functions.* Numer. Funct. Anal. Optim. **25**, 463–478, 2004.
[13] X. Bresson and T. F. Chan; *Fast dual minimization of the vectorial total variation norm and applications to color image processing.* Inverse Probl. Imaging **2**, 455–484, 2008.
[14] A. Buffa and C. Ortner; *Compact embeddings of broken Sobolev spaces and applications.* IMA J. Numer. Anal. **29**, 827-855, 2009.
[15] R. Bustinza and G. Gatica; *A local discontinuous Galerkin method for nonlinear diffusion problems with mixed boundary conditions.* SIAM J. Sci. Comput. **26**, 152-177, 2004.
[16] A. Chambolle; *An algorithm for total variation minimization and applications.* Journal of Mathematical Imaging and Vision **20**, 89–97, 2004.
[17] K. Yosida; *Functional Analysis.* Springer, Berlin-Heidelberg-New York, 1995.